

Steric stabilization of nanoparticles with grafted low molecular weight ligands in highly concentrated brines including divalent ions

**Andrew J. Worthen, Vu Tran, Kevin A. Cornell, Thomas M. Truskett, and Keith P. Johnston\***

McKetta Department of Chemical Engineering, University of Texas at Austin, Austin, Texas, USA

\* Corresponding Author: [kpj@che.utexas.edu](mailto:kpj@che.utexas.edu)

**Supporting Information**

The supporting information contains the calculation methodology for ligand coverage on NPs, additional details of the DLVO calculations, characterization of ligand solubility in brine, additional images of NP dispersions, tables of data shown in Figure 6, calculation of stability ratio  $W$ , and additional information on the effect of varying GLYMO coverage on NPs.

**Calculation of ligand coverage on NPs.** The ligand grafting density  $\phi_l$  ( $\mu\text{mol ligand} / \text{m}^2 \text{ NP surface}$ ) is calculated by equation S1

$$\phi_l = \frac{f_o}{(1-f_o)S_A M_{TGA}} * 10^6 \quad (\text{S1})$$

where  $f_o$  is particle organic fraction by TGA,  $S_A$  is particle specific surface area by BET given in Table S1, and  $M_{TGA}$  are given in Table S2. A full monolayer is assumed to be  $7.6 \mu\text{mol ligand} / \text{m}^2 \text{ NP surface}$  (equivalent to  $4.6 \text{ atoms/nm}^2$ , the typical density of reactive silanol sites on colloidal silica<sup>1</sup>). Thus monolayer fraction is given by  $\phi_l / 7.6$ .

Table S1. Measured surface area of bare nanoparticle samples via BET.

Nanoparticle	Measured Surface Area ( $\text{m}^2/\text{g}$ )
NexSil 6	410.8
NexSil 12	199.6
NexSil 20	119.5
NexSil 125	49.23
ST-UP	229.8
ST-O	237.0
ST-PS-S	174.6

Table S2. Molecular weight of ligand removable by TGA ( $M_{TGA}$ )

Ligand	$M_{TGA}$ (Da)
GLYMO	133
SB	208
PEG (6-9EO)	404
PEG (8-12EO)	500

$M_{TGA}$  is the molecular weight of the portion of the ligand removable by TGA (see Figure S5 for GLYMO example).

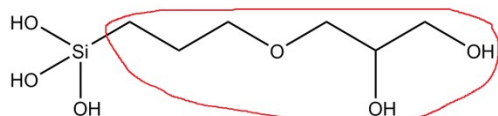
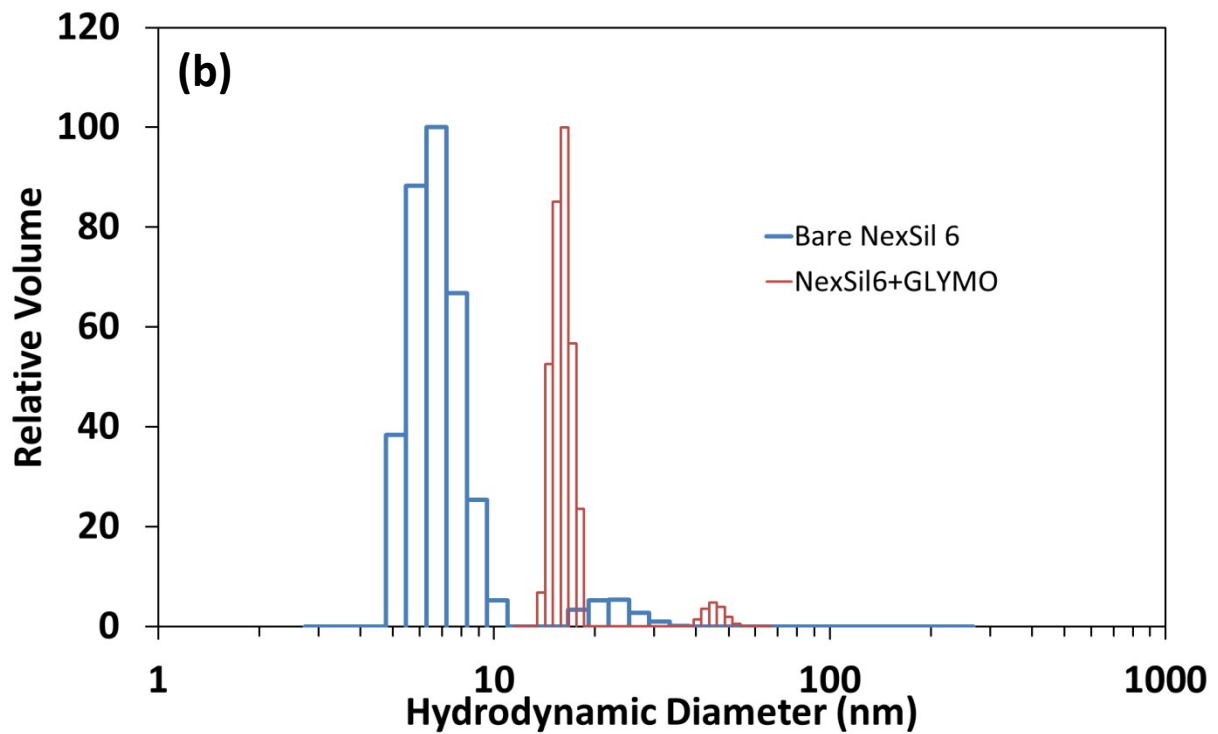
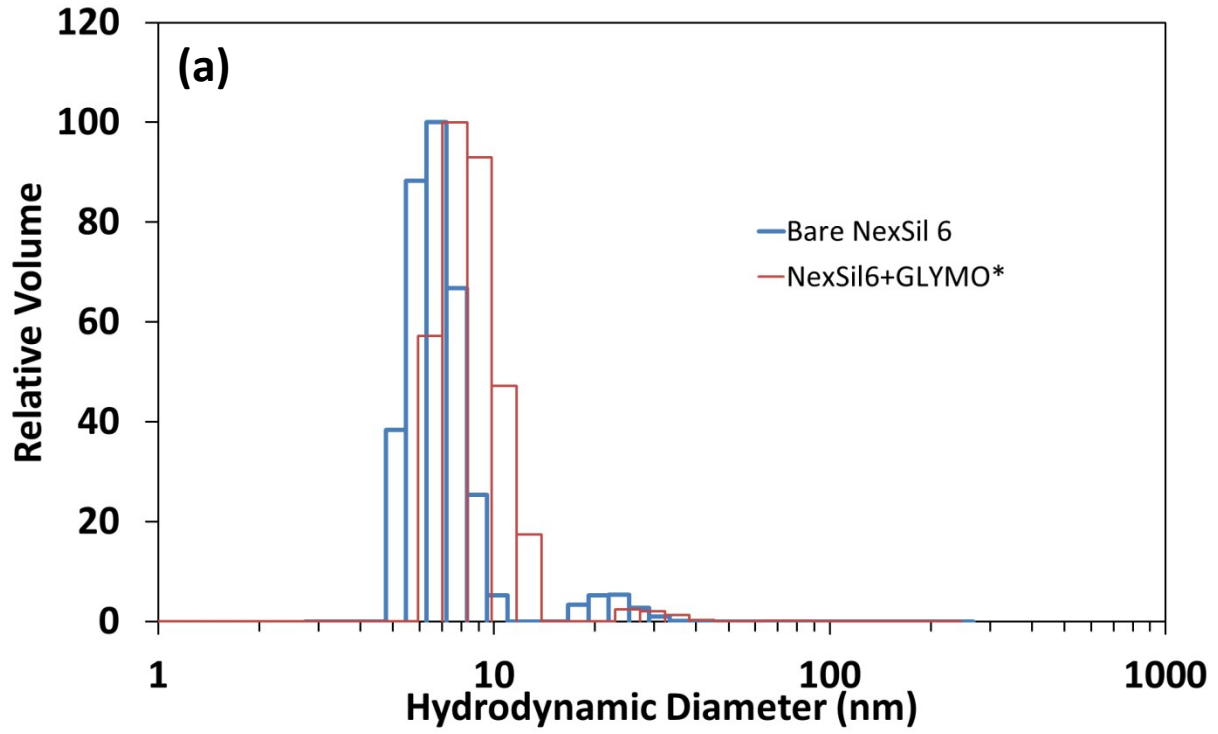
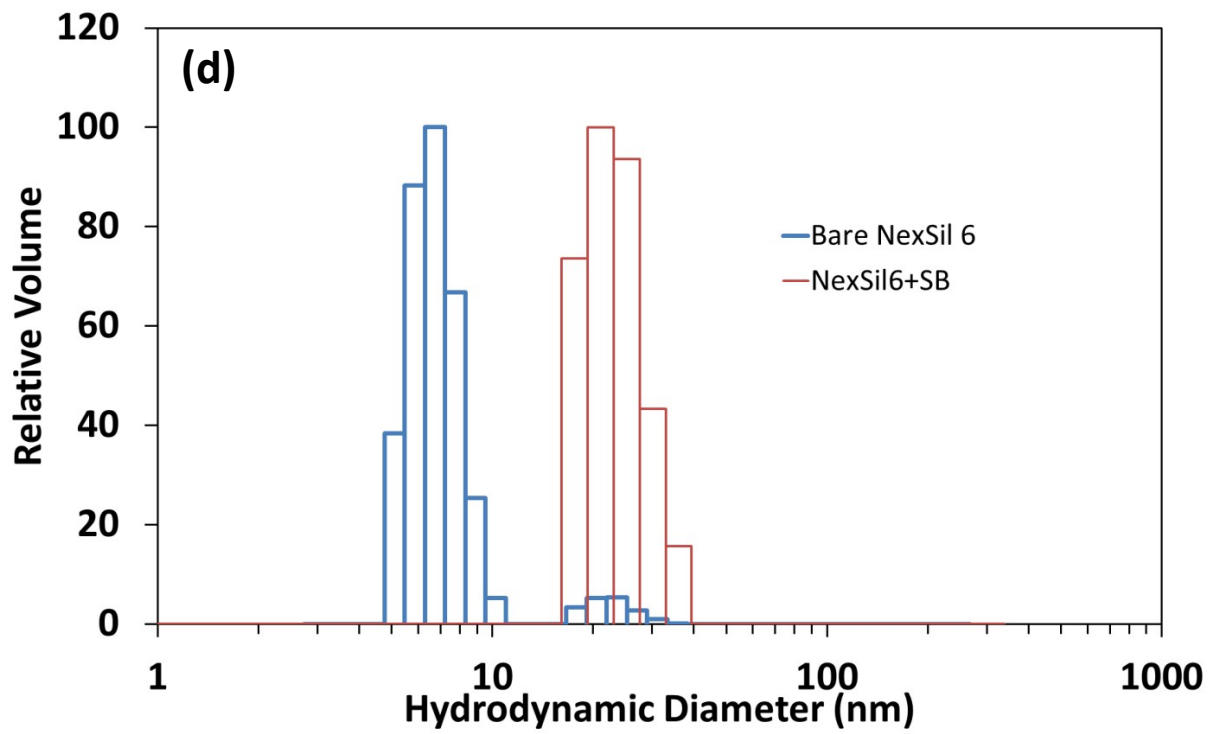
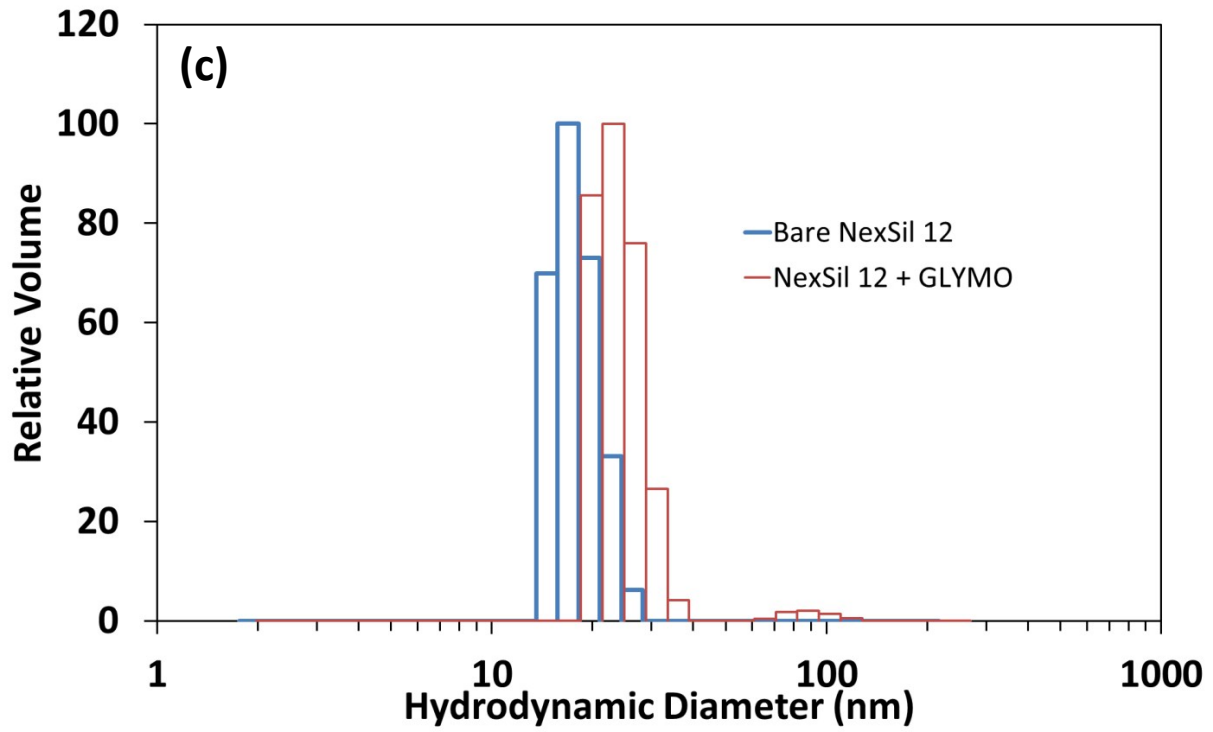


Figure S1. Portion of GLYMO removable by TGA encircled in red.

NP size distributions measured by dynamic light scattering (DLS)





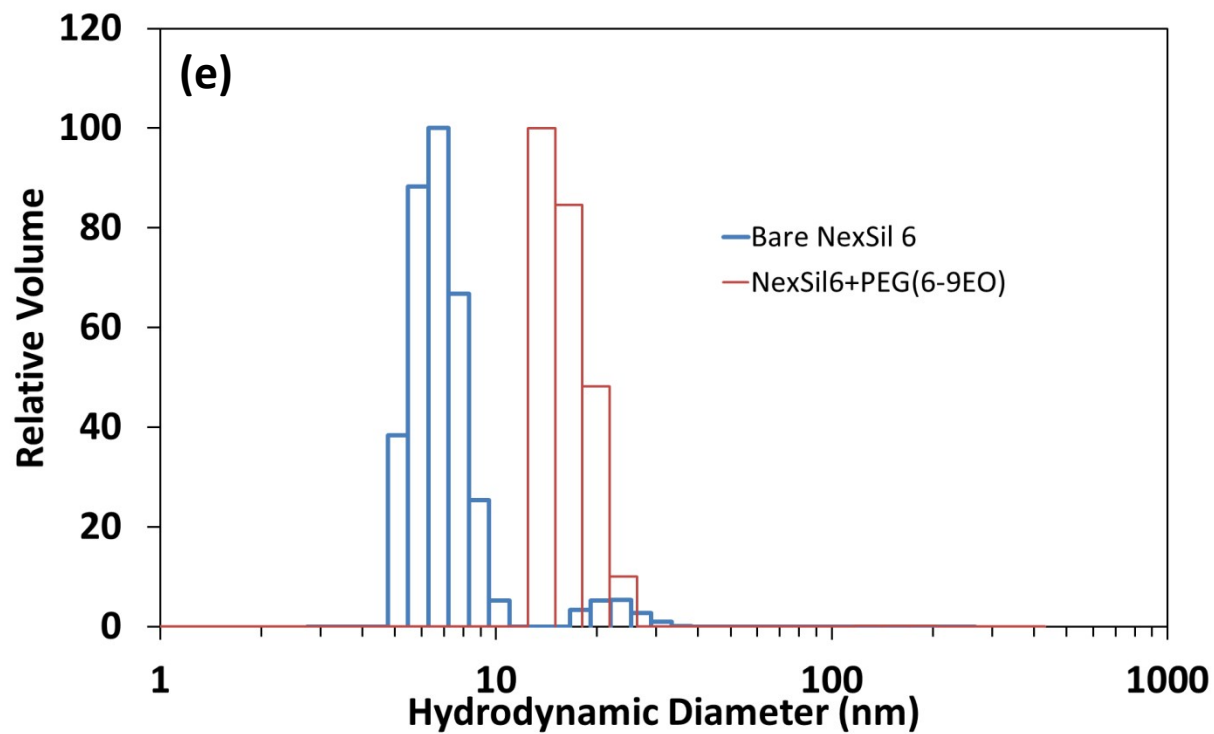


Figure S2. Representative DLS size distributions of NPs in DI water after purification.

#### Additional DLVO calculation information

Table S3. Parameters for DLVO calculation.

Parameter	Value
Particle diameter	16 nm
GLYMO length	0.95 nm
SB length	1.2 nm
Particle surface potential	-35 mV
Hamaker constant for water	$3.7 \cdot 10^{-20}$ J
Hamaker constant for silica	$6.3 \cdot 10^{-20}$ J
Bulk density of pure ligand	1 g/mL
Molecular weight of GLYMO	236 g/mol
Molecular weight of SB	329.5 g/mol

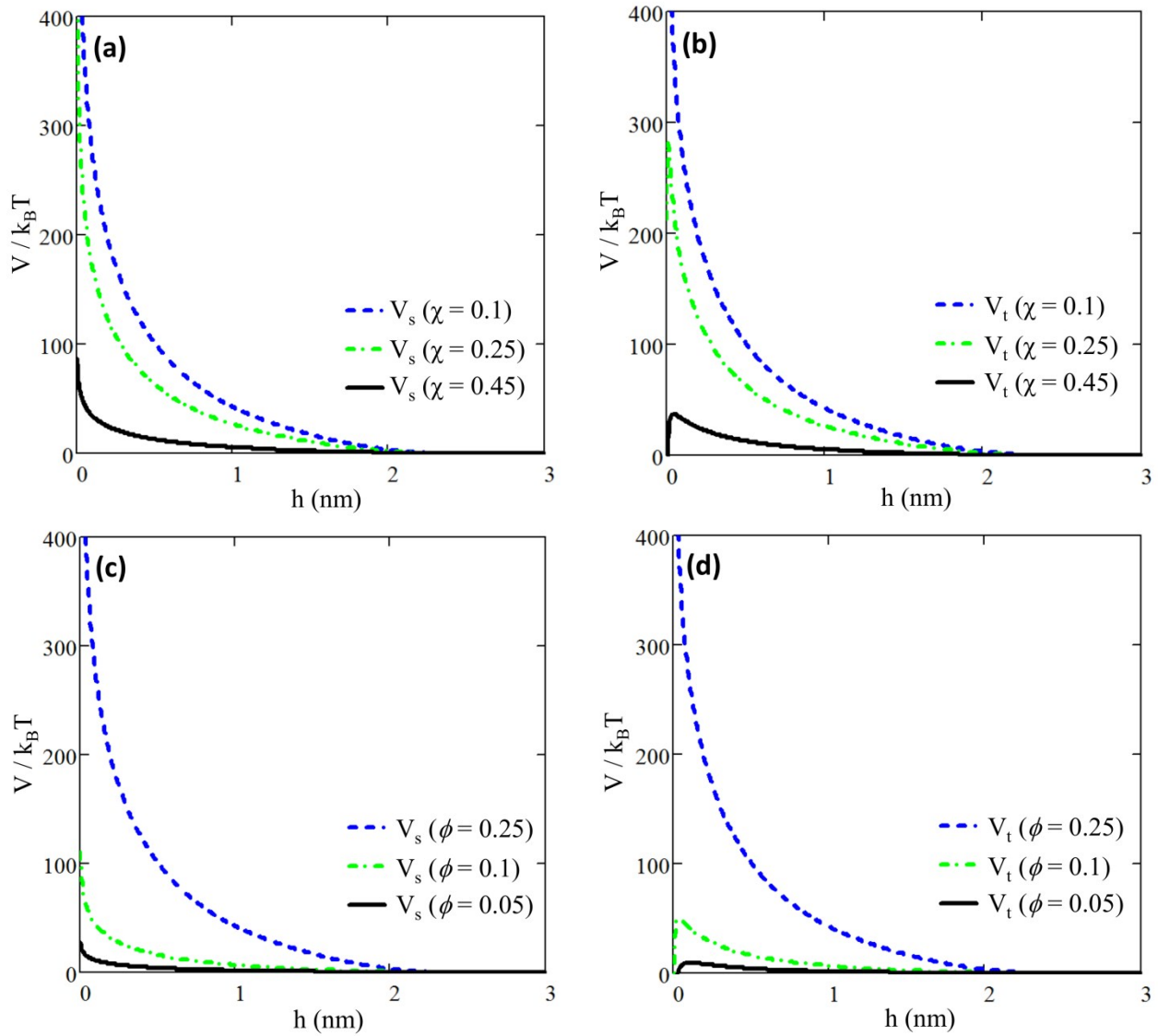


Figure S3. Interparticle interaction potential ( $V$ ) for 16 nm diameter SB-coated silica particle at pH 8 by extended DLVO calculations as a function of particle separation distance ( $h$ ). (a) Extended DLVO calculation of steric repulsion potential ( $V_s$ ) at Flory-Huggins  $\chi = 0.1, 0.25,$  and  $0.45,$  holding the ligand volume fraction  $\phi = 0.25.$  (b)  $V_t$  in API brine including  $V_a$  and  $V_r$  shown in Figure 8a as well as  $V_s$  shown in panel (a). (c)  $V_s$  at  $\phi = 0.05, 0.1,$  and  $0.25,$  holding  $\chi = 0.1.$  (d)  $V_t$  in API brine including  $V_a$  and  $V_r$  shown in Figure 8a as well as  $V_s$  shown in panel (c).

### Ligand solubility in brine.

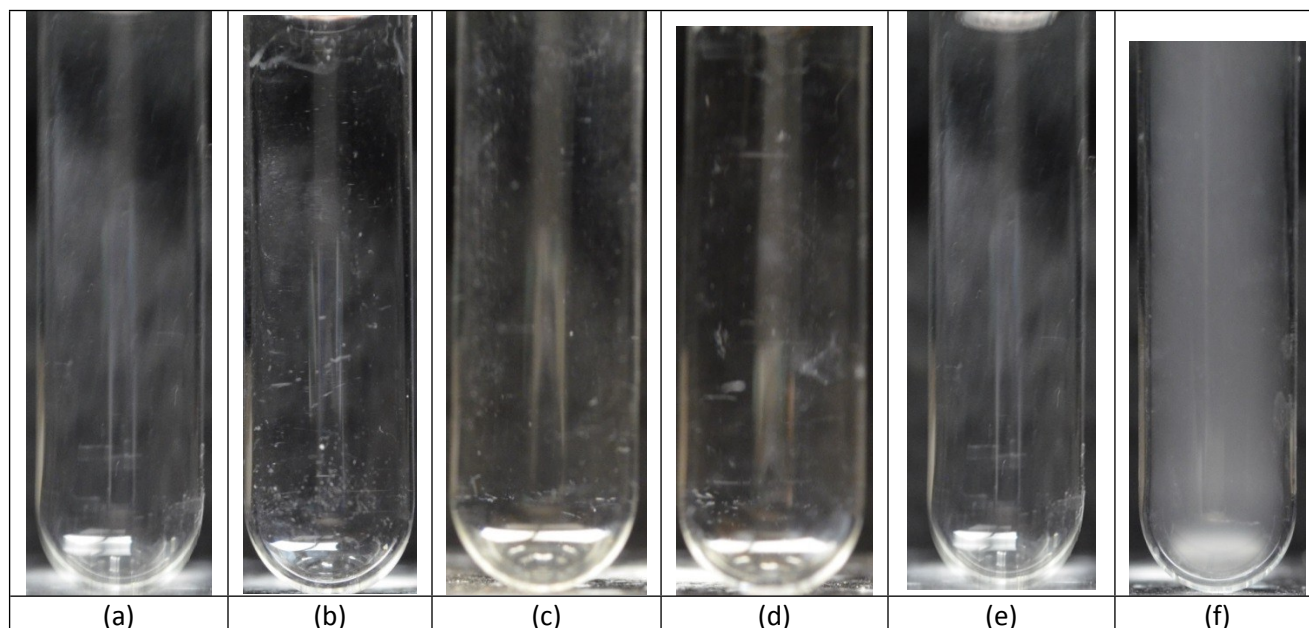


Figure S4. Photographs of solubility observations in API brine taken in front of a dark grey background immediately after removing sample from a 120°C oven. Images show 0.05% w/v solutions of (a) GLYMO, (b) SB, (c) PEG(6-9EO), (d) PEG(8-12EO), (e) 300 Da molecular weight PEG, (f) 8 kDa molecular weight PEG. All are clear except the 8 kDa PEG shown in panel (f). The pH was  $7 \pm 1$  in all samples. 300 Da PEG was also tested at concentrations of 0.5, 5, 10 and 30% in API brine and all were clear at 120°C. All images were taken less than 30 s after removal from the 120C oven and no changes were visually observed before photographs were taken.

### Additional NP stability characterization

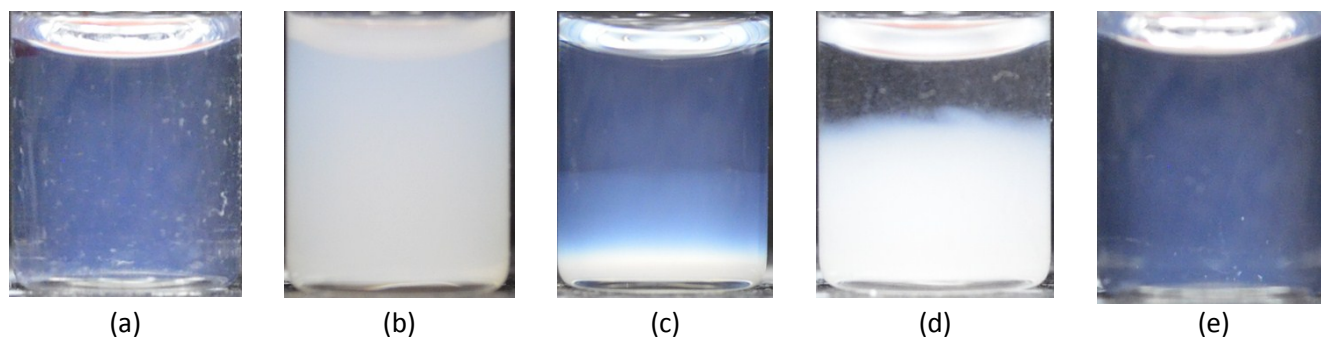


Figure S5. Macroscopic images of stability observations taken in front of a dark grey background for 0.5% w/v NPs including (a) stable dispersion of NexSil 6 + GLYMO at pH 3.5 in API brine at  $t = 720$  h, (b) strongly aggregated NexSil 6 + SB at pH 3.5 in DI water at  $t = 0$  h, (c) settled NexSil 125 + GLYMO particles at pH 3.5 in DI water at  $t = 720$  h, (d) aggregated and settled NexSil 6 + PEG(8-12EO) in pH 3.5 API brine after heating overnight at 80°C, and (e) redispersed NexSil 6 + PEG(6-9EO) after cooling below CFT. Vial outside diameter = 1.47 cm.

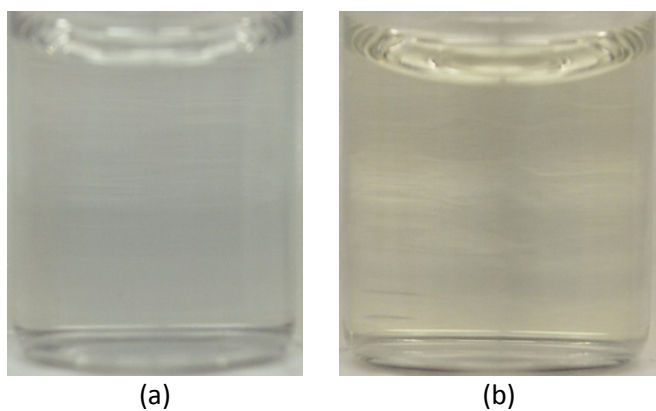


Figure S6. Macroscopic images of taken in front of a white background of after 60 days in pH 3.5 API brine at 80°C (a) NexSil 6 + GLYMO and (b) N6 + SB\*\*. The GLYMO sample showed no color change while the SB\*\* sample took on a yellow tint. Vial outside diameter = 1.47 cm.

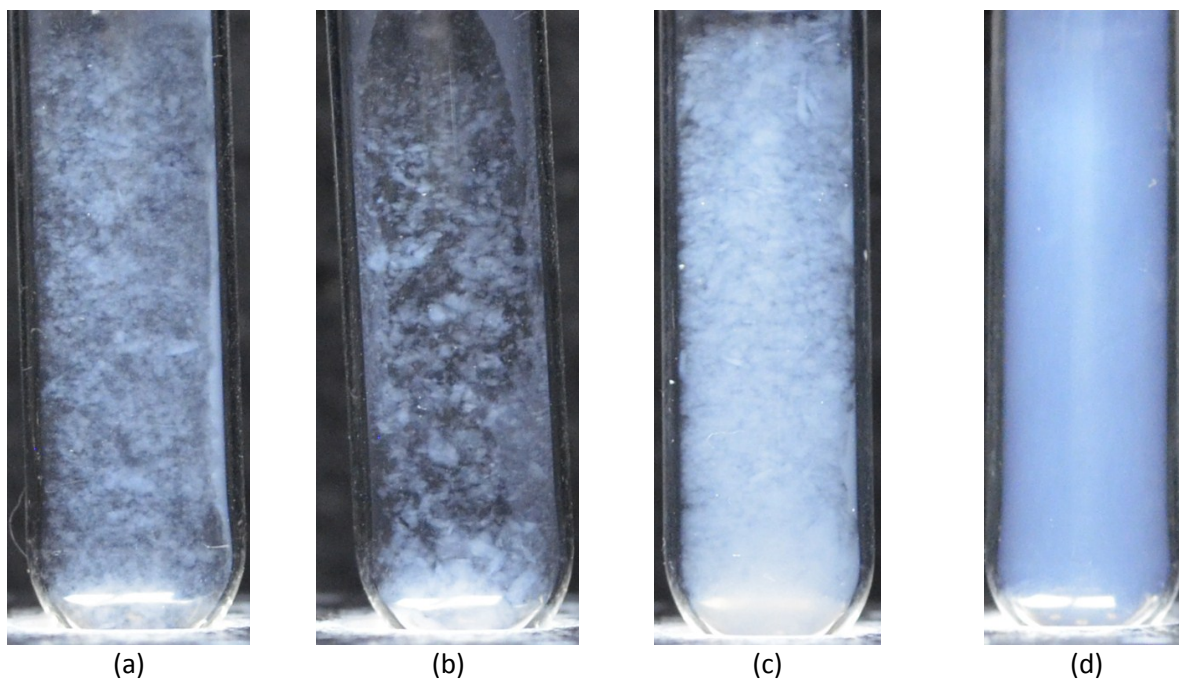


Figure S7. Macroscopic images taken in front of a black background after 3 days in API brine at 120°C of NexSil 6 + SB\*\* at pH 8 (a) and 3.5 (b) and NexSil 6 + GLYMO at pH 8 (c) and 3.5 (d). Note that these samples were agitated slightly before the pictures were taken. Vial outside diameter = 1.28 cm.

Table S4. Nanoparticle stability data collected via DLS measurements in pH 3.5 API brine at RT and 80°C with 0.5% w/v NPs.

Particle	RT			80°C		
	t(h)	size (nm)	standard deviation (nm)	t(h)	size (nm)	standard deviation (nm)
NexSil 6 + GLYMO*	0.1	9.8	1.2	36	9.1	1.5
	36	10.1	0.8	168	9.7	0.7
	168	9.5	0.5	720	9.6	1.3
	720	9.6	1.1			
NexSil 6 + GLYMO	0.1	17.8	1.5	24	18.6	3.1
	26	17.7	0.2	168	20.0	1.7
	336	16.2	2.2	720	21.32	3.6
	2352	17.2	1.7			
	6000	17.6	0.2			
NexSil 12 + GLYMO	0.1	30.9	2.1	24	29.9	6.5
	360	29.9	1.3	168	39.0	4.1
	1032	33.0	1.8	720	154.77	18
NexSil125 + GLYMO	0.1	92.1	4.8	24	129	7.7
	240	90.9	6.3	168	137	6.1
	2640	94.4	14	720	>1 micron	-
NexSil 6 + SB**	0.1	17.4	1.4	24	20.1	1.4
	1032	15.2	1.6	168	22.5	2.2
	4200	16.4	2.2	720	18.6	1.9
NexSil 6 + PEG (6-9EO)	0.1	18.0	2.7	1	>1 micron	-
	1464	16.2	4.9			
	5160	22.9	0.1			
NexSil 6 + PEG (8-12EO)	0.1	19.9	1.4	1	>1 micron	-
	96	18.3	3.0			
	720	18.5	1.5			

Table S5. Nanoparticle stability data collected via DLS measurements at higher temperature and salinity conditions with 0.5% w/v NPs.

Particle	T (°C)	Salinity	pH	t(h)	size (nm)	standard deviation (nm)
NexSil6 + GLYMO	RT	2xAPI brine	3.5	initial	20.0	1.7
	RT	2xAPI brine	3.5	48	22.0	1.5
	80	2xAPI brine	3.5	48	23.0	2.7
	80	>2xAPI brine	3.5	2640	51.5	8.9
	120	API	8-9	72	>1 micron	-
	120	API	3.5	72	54.0	3.7
NexSil 6 + SB**	RT	2xAPI brine	3.5	initial	22.5	2.2
	RT	2xAPI brine	3.5	48	29.2	9.7
	80	2xAPI brine	3.5	48	29.2	7.8
	120	API	8-9	72	>1 micron	-
	120	API	3.5	72	>1 micron	-

**Calculation of stability ratio W.** Colloidal stability was quantified based on the time-dependent hydrodynamic diameters measured by DLS. The Fuchs-Smoluchowski equation for monodisperse spheres gives the rate constant for rapid coagulation  $k_r$  as

$$k_r = \frac{8k_B T}{3\mu} \quad (S2)$$

and the rate of slow coagulation  $k_s$  as

$$k_s = \frac{k_r}{W} \quad (S3)$$

where  $k_B$  is the Boltzmann constant,  $T$  is the absolute temperature,  $\mu$  is the solvent viscosity, and  $W$  is the stability ratio<sup>2-3</sup>. The stability ratio  $W$  is related to the time required to reduce the initial particle number concentration  $N_0$  by half, known as the half-time  $t_{1/2}$ <sup>2-3</sup>.

$$t_{1/2} = \frac{3\mu W}{4k_B T N_0} \quad (S4)$$

From eqn. 3,  $W$  is calculated with the assumption that  $t_{1/2}$  equals the time when the average particle volume doubled (as measured by DLS), indicating that the number of particles was reduced by half.

To quantify the colloidal stability of the particles shown in Figure 6, the calculated stability ratio  $(W)^{2-3}$  for each sample is given in Table S5. In room temperature API brine, the calculated number of NPs did not decrease by  $\frac{1}{2}$  in the time-scale of the measurement (given in parenthesis below the calculated  $W$  value), so all  $W$  values are given as a lower limit. Thus, according to Equation S4, the differences in the calculated limiting values are only due to differences in (1) initial particle number concentration due to differences in particle size and (2) duration of observation, making quantitative comparison of particle stabilities difficult.

At 80°C, the  $W$  for the most stable NexSil 6 particles (those coated with GLYMO and SB+GLYMO) are also given as a lower limit. Note that as temperature increased, the solvent viscosity is reduced, allowing more particle movement, and thus the limiting calculated  $W$  is higher for a given stable particle at a given time compared to room temperature. At 80°C, NexSil 12 + GLYMO and NexSil 125 + GLYMO aggregated rapidly enough to have a measurable  $t_{1/2}$ , while the PEG-coated particles aggregated too rapidly for accurate measurement (in under 1 minute) and the given  $W$  is an upper bound. At 120°C, aggregation (but no settling) of GLYMO-coated particles is quantified by a much lower  $W$ . The stability of SB-coated particles was even lower than the GLYMO-coated particles, where an aggregated gel-like phase was produced after 72h. Dong and coworkers<sup>2</sup> calculated  $W$  values of  $5.2 \times 10^5$  to  $8.3 \times 10^6$  for 1% 150nm copper phthalocyanine particles which slowly aggregated (but did not gravity settle) over the course of weeks in a surfactant solution.

Table S6. Stability ratio  $W$  calculated from DLS data given in Figure 6 and Tables S1-S2. Note that most are given as a lower or upper bound if the particles did not measurably aggregate in the time investigated or aggregated beyond DLS sizing range too rapidly to accurately quantify, respectively.

Particle	$W$ @ RT (half-time, h)	$W$ @ 80°C (half-time, h)	$W$ @ 120°C (half-time, h)
NexSil 6 + GLYMO*	$>3.6 \times 10^{11}$ ( $>720$ )	$>7.1 \times 10^{11}$ ( $>720$ )	-
NexSil 6 + GLYMO	$>5.0 \times 10^{11}$ ( $>6000$ )	$>1.2 \times 10^{11}$ ( $>720$ )	$<3.4 \times 10^{10}$ ( $<72$ )
NexSil 12 + GLYMO	$>1.6 \times 10^{10}$ ( $>1032$ )	$5.3 \times 10^9$ (168)	-
NexSil125 + GLYMO	$>1.6 \times 10^9$ ( $>2640$ )	$2.9 \times 10^7$ (24)	-
NexSil 6 + SB**	$>3.8 \times 10^{11}$ ( $>4200$ )	$>1.3 \times 10^{11}$ ( $>720$ )	$<<3.7 \times 10^{10}$ ( $<<72$ )
NexSil 6 + PEG (6-9EO)	$>4.1 \times 10^{11}$ ( $>5160$ )	$<1.6 \times 10^6$ ( $<0.01$ )	-
NexSil 6 + PEG (8-12EO)	$>4.3 \times 10^{10}$ ( $>720$ )	$<1.2 \times 10^6$ ( $<0.01$ )	-

#### Variation of GLYMO ligand coverage on NPs

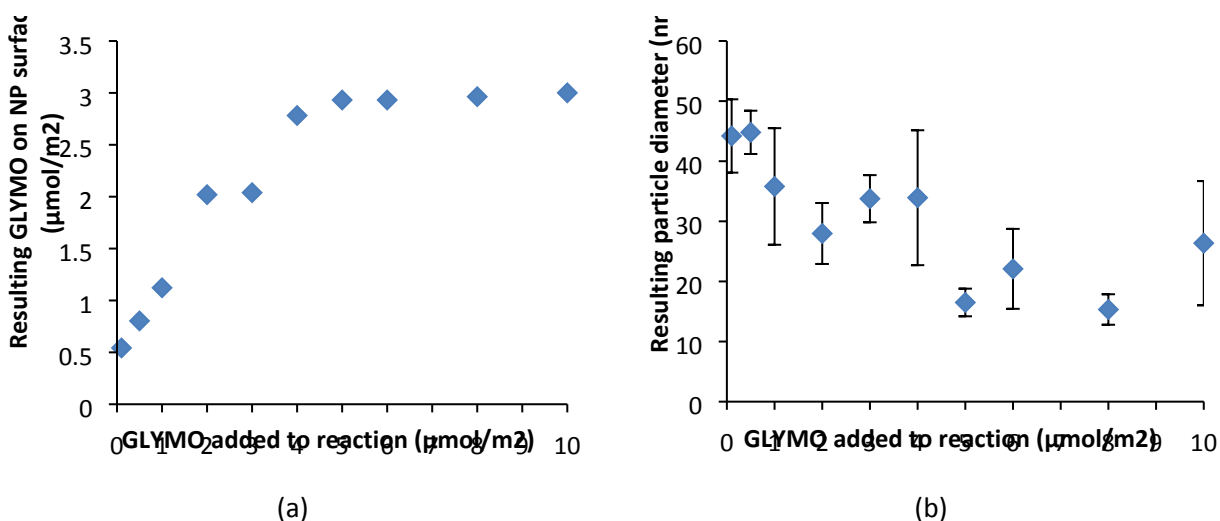


Figure S8. Variation of GLYMO added to the reaction mixture affecting resulting (a) GLYMO on NP surface (determined by TGA) and (b) initial NP particle size in DI water (determined by DLS).

1. Bergna, H. E. Colloid Chemistry of Silica: An Overview. In *Colloidal Silica: Fundamentals and Applications*, Bergna, H. E.; Roberts, W. O., Eds.; CRC Press: Boca Raton, 2006; Vol. 131, p 9.

2. Dong, J.; Chen, S.; Corti, D. S.; Franses, E. I.; Zhao, Y.; Ng, H. T.; Hanson, E. Effect of Triton X-100 on the stability of aqueous dispersions of copper phthalocyanine pigment nanoparticles. *Journal of Colloid and Interface Science* **2011**, 362 (1), 33-41.
3. Hiemenz, P., C.; Rajagopalan, R. *Principles of Colloid and Surface Chemistry*; Third ed.; Taylor & Francis Group, LLC: Boca Raton, FL, 1997.